Impact of Time Reversal on Multi-User Interference in IR-UWB

Jocelyn Fiorina[*], Guido Capodanno[†], Maria-Gabriella Di Benedetto[†]

[*]SUPELEC, TELECOM Dept., France.

[†]University of Rome "La Sapienza", INFOCOM Dept., Italy.

Abstract—**In this paper we investigate the use of Time Reversal applied to Impulse Radio Ultra Wide Band (IR-UWB) systems with multi user interference (MUI). It is known that the MUI distribution is often not Gaussian in classical IR-UWB. We show how the Time Reversal technique has an impact on the distribution of the multi-user interference (MUI) by making it even less Gaussian. So we show how performance may benefit from this MUI distribution change.**

I. Introduction

The first studies on Time Reversal technique (TR) were done in the field of acoustic [4] [2]. It has then been proposed for radio telecommunication systems and has been applied to Impulse Radio Ultra Wide Band systems (IR-UWB) in various works [1] [6] [5]. The basic idea was to exploit the spatial and temporal focusing properties of Time Reversal and to benefit also from the switch of complexity from the receiver to the transmitter. As a matter of fact, the role of a complex full rake receiver in a traditional system could be replaced by the combination of the time reversal transmitter prefilter convolved with the propagation channel. However in this paper, we investigate another face of Time Reversal: its impact on the multi user interference (MUI) distribution. We show that by applying Time Reversal to Impulse Radio Ultra Wide Band systems we can change the MUI distribution, and by adapting the reception to this distribution change wa can increase the performance. The Time Reversal MUI is more favorable than classical MUI.

In section II we will give the signal model used in all the paper. We will see in section III how the distribution of the MUI is affected by Time Reversal. It has been already shown that the Standard Gaussian Approximation (SGA) is often not valid in calssical IR-UWB [12] [3] [17], we show that the SGA is even less accurate if we use TR. As the non Gaussianity of the interference can be turned into an advantage [18], we will see how we can benefit from the change in the MUI distribution brought by TR. In section IV we will check and quantify our claims through simulations.

II. Signal Model

The common signal model that we will consider in this paper is TH-IR UWB (Time Hopping Impulse Radio Ultra Wide Band) signal using PAM (Pulse Amplitude Modulation) as well as PPM (Pulse Position Modulation). The classical (no TR) IR-UWB signal with PAM may be written as:

$$s_{noTR}(t) = \sqrt{E_s} \sum_m a_m w(t - mT_f - c_m T_c) \qquad (1)$$

In this expression, $w(t)$ is the unit-energy basic pulse waveform with a time support included in $[0, T_c)$, E_s is the energy sent per pulse, a_m the information symbol at symbol interval m, having its values in the set $\{-1, 1\}$. The so-called frame time is $T_f = N_h T_c$, where T_c is the so-called chip time interval (N_h is the frame length in chips). The time hopping code is represented by the sequence $(c_l)_{l \in \mathbb{Z}}$, the elements of which belong to $\{0, \ldots, N_h - 1\}$.

The classical (no TR) IR-UWB signal with PPM may be written as:

$$s_{noTR}(t) = \sqrt{E_s} \sum_m w(t - mT_f - c_m T_c - d_{PPM}(\frac{a_m + 1}{2})) \tag{2}$$

where d_{PPM} is the time shift used by the pulse position modulation.

We consider also a multipath channel $h(t)$:

$$h_k(t) = \sum_{i=1}^{L} \gamma_{k,i} \delta(t - \tau_{k,i}) \tag{3}$$

with L the total number of paths in the channel, τ_i the delay of the $i - th$ path and γ_i its amplitude.

By considering, without loss of generality a PAM signal, the received signal without TR may be written:

$$r_{noTR}(t) = \sqrt{\frac{E_r}{A}} \sum_m a_m h(t) * w(t - mT_f - c_m T_c) + n(t) \tag{4}$$

where $A = \int |h(t) * w(t)|^2 \, dt$ is only a normalization factor in order to let E_r represent the energy received per pulse. $n(t)$ is the Additive White Gaussian Noise (AWGN).

The idea in Time Reversal is to convolve the pulse with an inverted version of the channel before to send it. Thanks to this operation, during the propagation the convolution of the signal with the channel will have the effect to receive the channel correlated to itself (thus simulating a correlation receiver). So, the sent signal in Time Reversal may be written as:

$$s(t) = \sqrt{\frac{E_s}{\int |h_{in}(t) * w(t)|^2 \, dt}} \sum_m a_m h_{in}(t) * w(t - mT_f - c_m T_c) \tag{5}$$

E_s represents the energy sent by pulse, $h_{in}(t)$ is the prefilter. In case of perfect Time Reversal (or *full* TR) $h_{in}(t) = h(-t)$.

In order to reduce the complexity of the transmitter we may use a *partial* Time Reversal by reducing the number of path considered in $h_{in}(t)$, selecting only the N_{in} strongest paths of $h_{(t)}$ ($N_{in} = 1$ is equivalent to no TR):

$h_{in}(t) = \sum_{i=1}^{N_{in}} \gamma_i' \delta(-(t - \tau_i'))$, where τ_i' and γ_i' are the delay and amplitude of the strongest paths.

The received signal is then written:

$$r(t) = \sqrt{\frac{E_r}{\int |h(t) * h_{in}(t) * w(t)|^2 \, dt}} \cdot$$
$$\sum_m a_m h(t) * h_{in}(t) * w(t - mT_f - c_m T_c) + n(t) \tag{6}$$

We call $g(t) = h(t) * h_{in}(t)$ the equivalent Time Reversal channel. It is the concatenation of the transmission pre-filter and the multipath channel.

At the receiver side, we can use a rake receiver. A rake receiver has to perform the correlation of the received signal with a template $v(t)$. Without Time Reversal the rake receiver output for symbol n may be written:

$$r_{noTR}[n] = \int r_{noTR}(t).v_{noTR}(t - n.T_f - c_n T_c) dt \tag{7}$$

For a one finger rake receiver, we will have $v_{noTR}(t) = w(t)$ for a PAM signal and $v_{noTR}(t) = w(t) - w(t - d_{PPM})$ for a PPM signal. For an all rake receiver we will have $v_{noTR}(t) = h(t) * w(t)$ for a PAM signal and $v_{noTR}(t) = (h(t) * (w(t) - w(t - d_{PPM})))$ for a PPM signal. For a partial rake receiver we will have $v_{noTR}(t) = h_{out}(t) * w(t)$ for a PAM signal and $v_{noTR}(t) = (h_{out}(t) * (w(t) - w(t - d_{PPM})))$ for a PPM signal, where $h_{out}(t)$ is a subselection of the N_{out} strongest path of $h(t)$.

With Time Reversal the rake receiver output for symbol n may be written:

$$r[n] = \int r(t).v(t - n.T_f - c_n T_c) dt \tag{8}$$

For a one finger rake receiver, we will have $v(t) = w(t)$ for a PAM signal and $v(t) = w(t) - w(t - d_{PPM})$ for a PPM signal. For an all rake receiver we will have $v(t) = g(t) * w(t)$ for a PAM signal and $v(t) = (g(t) * (w(t) - w(t - d_{PPM})))$ for a PPM signal, with $g(t) = h(t) * h_{in}(t)$. For a partial rake receiver we will have $v(t) = h_{out}(t) * w(t)$ for a PAM signal and $v(t) = (h_{out}(t) * (w(t) - w(t - d_{PPM})))$ for a PPM signal, where $h_{out}(t)$ is a subselection of the N_{out} strongest path of $g(t)$.

III. TIME REVERSAL WITH MULTI USER INTERFERENCE

As we focus on the effect of Time Reversal in a communication with MUI, we consider the reception of unsynchronized signals at a receiving point which could be a base station for instance. Those unsynchronized signals focusing to the same geographical point with Time Reversal create MUI. Two basic topologies examples are given in Fig. 1 and Fig. 3.

We will investigate the distribution of this MUI and the impact of TR on it. In order to exploit the effect of the distribution change in the MUI, we will introduce a classical repetition code as it helps to simply exhibit the gain brought by non Gaussian MUI, but other channel codes could be envisaged [18].

The signal model of section II may be simply extended to the case where there are many users. With Time Reversal the signal coming from user k and received by the common receiver can be written in PAM :

$$r_k(t) = \sqrt{\frac{E_{r,k}}{\int |h_{in,k}(t) * w(t) * h_k(t)|^2 \, dt}} \cdot$$
$$\sum_m \sum_{j=0}^{Ns-1} a_{m,k} h_{in,k}(t) * w(t - (mN_s + j)T_f - c_{mN_s+j,k} T_c)$$
$$* h_k(t) \tag{9}$$

where N_s is the repetition factor. h_k is the channel from user k to the receiver, $h_{in,k}(t)$ is the user k TR pre-filter (subselection of the $N_{in,k}$ strongest path of $h_k(t)$), $c_{m,k}$ is the time hopping code of user k, the mth symbol that it sends is $a_{m,k}$ and the energy received by pulse is E_r, k.

While the signal received in PPM is written :

$$r_k(t) = \sqrt{\frac{E_{s,k}}{\int |h_{in,k}(t) * w(t) * h_k(t)|^2 \, dt}} \cdot$$
$$\sum_m \sum_{j=0}^{Ns-1} (h_{in,k}(t)$$
$$* w(t - (mN_s + j)T_f - c_{mN_s+j,k} T_c - d_{PPM}(\frac{a_{m,k} + 1}{2}))$$
$$* h_k(t)) \tag{10}$$

Thus, there are N_s pulses by symbol. In order to take a decision on the received symbol the rake receiver will have to collect N_s correlator outputs. Without loss of generality we consider the symbol $m = 0$ and we will consider a reception synchronized on user 1 so we will drop this index for this user. The output of the pulse-by-pulse correlator can be written as:

$$r_{imp}[n] = \int r_x(t).v(t - n.T_s - c_{1,n} T_c) dt \tag{11}$$

and we will collect the N_s outputs $r_{imp}[0]$ to $r_{imp}[N_s - 1]$ in order to decide the received symbol.

For PAM we will have $v(t) = h_{out}(t) * w(t)$ and for PPM we will have $v(t) = (h_{out}(t) * (w(t) - w(t - d_{PPM})))$ where $h_{out}(t)$ is a subselection of the N_{out} strongest path of $g(t) = h(t) * h_{in}(t)$.

$r_x(t)$ is the received signal:

$$r_x(t) = r_1(t) + r_{MUI}(t) + n(t). \qquad (12)$$

$$r_{MUI}(t) = \sum_{k=2}^{K} r_k(t - \Delta_k) \qquad (13)$$

is the multi user interference where Δ_k represents the relative delay of user k with respect to the reference signal of user 1, due to the absence of synchronization between the various users.

The classical receiver (adapted to Gaussian intereference but not adapted to other distribution) will make its decision for the received symbol based on the sign of $\sum_{n=0}^{n=N_s-1} r_{imp}[n]$. So it operates a soft decision on the bit received.

The pulse-by-pulse correlator output can be decomposed as follows:

$$r_{imp}[n] = r_{imp,u}[n] + r_{imp,MUI}[n] + r_{imp,AWGN}[n] \qquad (14)$$

with $r_{imp,u}[n] = \int r_1(t).v(t - n.T_s - c_{1,n}T_c)dt$ being the useful signal contribution,
$r_{imp,MUI}[n] = \int s_{MUI}(t).v(t - n.T_s - c_{1,n}T_c)dt$ is the MUI contribution, and
$r_{imp,AWGN}[n] = \int n(t).v(t - n.T_s - c_{1,n}T_c)dt$ is the AWGN contribution.

In the following we will look at the distribution of the MUI contribution $r_{imp,MUI}[n]$.

It has been proved that MUI distribution is not Gaussian in several cases [3] [17]. We want to show that the standard Gaussian approximation is even less accurate if we consider a UWB-IR transmisssion scheme that makes use of Time Reversal. In this case, MUI distribution is more and more far from a Standard Gaussian if the TR technique approaches the *full* TR, that is if the number of fingers of transmission pre-filters N_{in} grows. We consider the kurtosis $k = \frac{E[r_{imp,MUI}[n]^4]}{E[r_{imp,MUI}[n]^2]^2} - 3$ of the MUI distribution as the reference parameter. The Kurtosis is a measure of how far a distribution is from the Gaussian distribution, the kurtosis of the normal distribution being 0. It has been shown in [17] that the non validity of the Gaussian approximation is due to the impulsivness of the MUI. Time Reversal increases this impulsivness as it focus the peak of the signal in time.

While the non Gaussianity of the MUI is a problem when a classical receiver is used, it has been shown in [18] that, for the same MUI power and using an adapted reception, it becomes more advantageous when the MUI is farther from classical Gaussian.

The Time Reversal effect on the MUI distribution has been confirmed in our simulations: as expected, when the number of fingers of the transmission pre-filter increases, the impact of TR is more significant and the kurtosis of the MUI distribution

is farther from 0, so the MUI is farther from classical Gaussian as it can be seen in the histograms of Fig. 4. The details of the simulations will be exposed in the section IV.

As the standard Gaussian approxiamtion is not appropriate, we use the Generalized Gaussian to better fit the MUI distribution [18]. The expression of this distribution is given by:

$$p(x) = \frac{c_1(\beta)}{\sqrt{\sigma^2}} exp(-c_2(\beta) \left| \frac{x}{\sqrt{\sigma^2}} \right|^{\frac{2}{1+\beta}})$$

with

$$c_1(\beta) = \frac{\Gamma^{\frac{1}{2}}(\frac{3}{2}(1+\beta))}{(1+\beta)\Gamma^{\frac{3}{2}}(\frac{1}{2}(1+\beta))}$$

and

$$c_2(\beta) = (\frac{\Gamma(\frac{3}{2}(1+\beta))}{\Gamma(\frac{1}{2}(1+\beta))})^{\frac{1}{1+\beta}}$$

The relation between the kurtosis k and the coefficient β is given by:

$$k = \frac{\Gamma(\frac{5(1+\beta)}{2})\Gamma(\frac{(1+\beta)}{2})}{(\Gamma(\frac{3(1+\beta)}{2}))^2} = \aleph(\beta)$$

A receiver adapted to a Generalized Gaussian interference has been exposed in [7]. This receiver consists in the insertion of a non-linear limiter that takes into account the parameter $\beta = \aleph^{-1}(k)$ [7]. Then, the expression of the limiter function h_l is:

$$h_l(x) = (|x+1|^{\frac{2}{1+\beta}} - |x-1|^{\frac{2}{1+\beta}})$$

The adapted receiver will make its decision for the received symbol based on the sign of $\sum_{n=0}^{n=N_s-1} h_l(r_{imp}[n]/E_r)$.

IV. SIMULATIONS

In the first scenario that we have considered in our simulations there are 12 users distributed in the network according to a star topology (see Fig. 1), where the distance from the transmitters to the receiver is 10 meters. All users transmit Time Reversal PPM-TH-UWB signals with the same power, but the channels h_k are different for each user. The channel model that we have used in our simulation is the model of reference IEEE 802.15.3a channel [14]. The chip time has been chosen to be $T_c = 2ns$, the shift used in the PPM modulation is $d_{PPM} = 0.5ns$ and the number of slots per frame is $N_h = 24$. For $w(t)$ we use the Scholtz's pulse (15):

$$w(t) = \left[1 - 4\pi \left(\frac{t}{T_c}\right)^2\right] \cdot exp\left[-2\pi \left(\frac{t}{T_c}\right)^2\right]. \qquad (15)$$

In Fig. 2, we show the histogram of the distribution of the multi-user interference $r_{imp,MUI}$ resulting from the simulations for a case with ($N_{in} = 10$, $N_{out} = 20$) and for a case with ($N_{in} = 20$, $N_{out} = 20$) approaching more the full TR. The kurtosis is also reported.

As expected, by increasing the number of fingers in the pre-filter, the kurtosis is farther from 0: the MUI distribution differs further from a Gaussian.

Then we have verified that the non-Gaussianity of the distribution is even more important in a worst case network
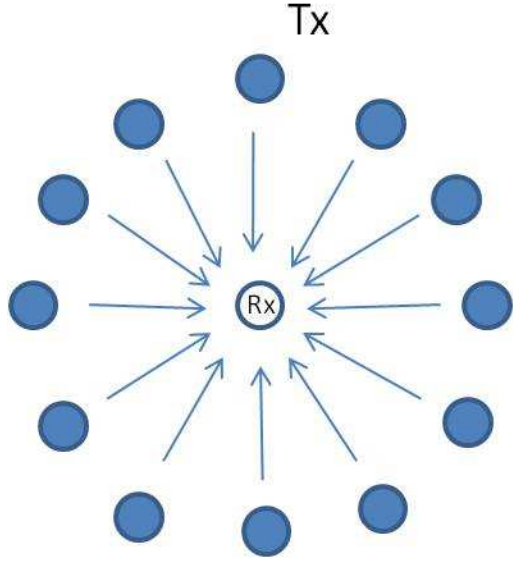
Fig. 1. Star Topology

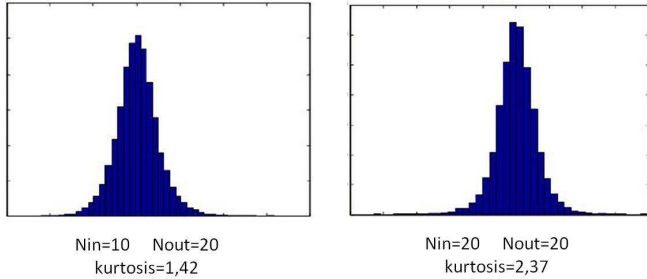Nin=10   Nout=20
kurtosis=1,42

Nin=20   Nout=20
kurtosis=2,37

Fig. 2. Histogram of the MUI ($r_{imp,MUI}$) with its kurtosis, illustrating the impact of time reversal on the non Gaussianity of the MUI distribution.

topology of reference: the ring topology [15] (see Fig. 3). We consider 30 transmitting users on a circle, the intended transmitter user 1 suffers from the interference of the other transmitters and user 1 is located at the maximum distance (at the opposite place on the circle) from the receiver.

In the simulation the repetition factor is $N_s = 6$, the diameter of the ring is 10 meters, the symbol interval is $T_s = N_h.T_c = 96$ ns, and the chip interval is still T_c to 2 ns. The power transmitted by each user is the same, while the received powers depend on the channel and distance from the receiver. The Bit Error Rate (BER) has been evaluated once that at least 100 wrong bits were received. In Fig. 4 the results are shown: we have plotted the pulse-by-pulse $r_{imp,MUI}[n]$ distribution with the respective performance in terms of BER vs. SNR, with $N_{out} = 10$ and with various N_{in}. At high SNR the AWGN is negligible and there is a BER floor created only by the interference.

As we can see in Fig. 4, when we approach full TR (by increasing N_{in})), the kurtosis of r_{MUI} increases and the performance achieved by the adapted receiver increases.

Then we consider the use of an All Rake receiver ($N_{out} = all$).
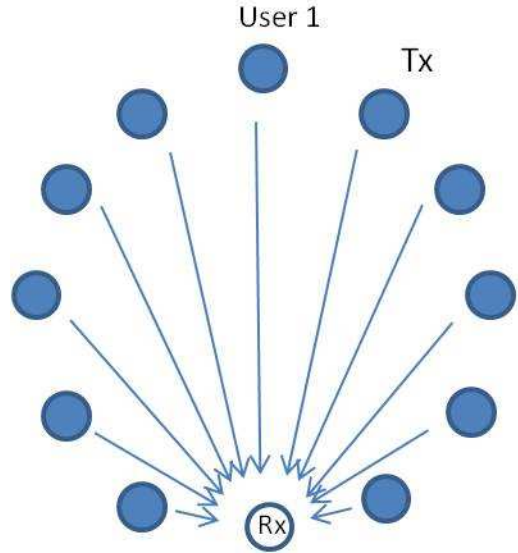

Fig. 3. Ring Topology. ("'worst case"' topology of reference [15]). On this figure there are only 11 transmitting users.

We have shown in Fig. 5 the difference of performance when no Time Reversal is used and a classical receiver is used, and when we use a complete TR configuration with the receiver adapted to the Generalized Gaussian distribution fitting the new MUI distribution. This underlines the gain brought by the exploitation of the MUI distribution change due to TR.

V. CONCLUSIONS

We have seen how the focussing properties of Time Reversal can be used in TH-IR-UWB communications with Multi User Interference. TR makes the multi user interference more impulsive, with a thighter distribution and a higher kurtosis. The parameters that tune the quality of the Time Reversal are the number of fingers in the transmit pre-filter and the number of fingers in the rake receiver (related respectively to the complexity of the transmitter and of the receiver). As the non Gaussianity of the MUI turns to be an advantage, the change in the MUI distribution due to the Time Reversal can be exploited and brings clear improvements to the performance.

REFERENCES

[1] Abiodun E. Akogun and Robert C.Qiu and Nan Guo,"Demonstrating Time Reversal in Ultra-wideband Communications Using Time Domain Measurements",51st International Instrumentation Symposium, 8-12 May 2005, Knoxville, Tennessee
[2] Derode, A. and Roux,P. and Fink,M.,"Robust acoustic time reversal with high-order multiple scattering", Phys. Rev. Letters, 1995, pp. 4206-4209, vol.75
[3] Durisi, G. and Romano, G.,"On the Validity of Gaussian Approximation to Characterize the Multiuser Capacity of UWB TH-PPM", IEEE Conf. on Ultra Wideband Systems and Technologies,2002
[4] Fink, Mathias, "Time-reversal waves and super resolution", Journal of Physics: Conference Series 124 (2008), 4th AIP International Conference and the 1st Congress of the IPIA
[5] Liu,X. and Wang,B.-Z. and Xiao,S. and Deng.,J.,"Performance of Impulse Radio UWB communications based on Time Reversal Technique", Progress In Electromagnetics Research, PIER 79, 2008,pp.410-413
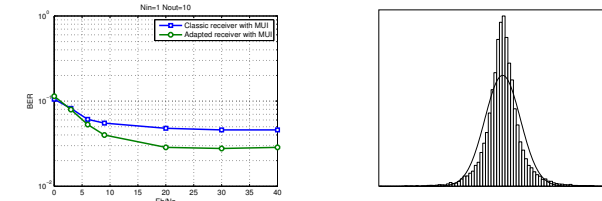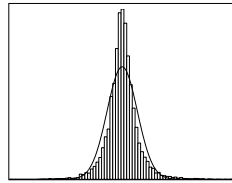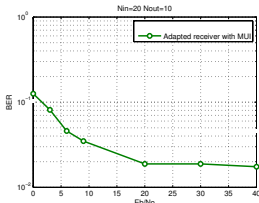
(a) BER vs. SNR with $N_{in} = 1, N_{out} = 10$
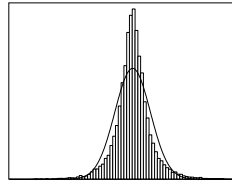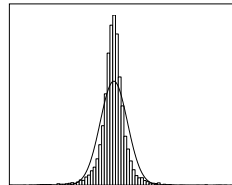
(b) $Kurtosis = 3.5$
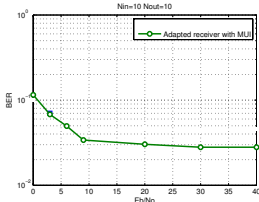
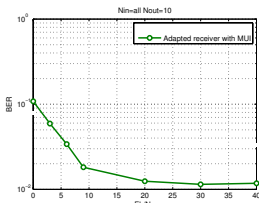(c) BER vs. SNR with $N_{in} = 10, N_{out} = 10$
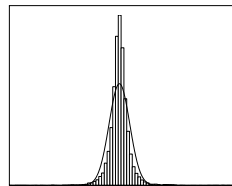
(d) $Kurtosis = 4.1$

(e) BER vs. SNR with $N_{in} = 20, N_{out} = 10$

(f) $Kurtosis = 9.8$

(g) BER vs. SNR with $N_{in} = all, N_{out} = 10$

(h) $Kurtosis = 17.6$

Fig. 4. Bit Error Rate performance (left); Histograms showing the distributions of the MUI $r_{imp,MUI}$ and superposition with a Gaussian probability density function having the same variance in order to underline the non-Gaussianity (right).
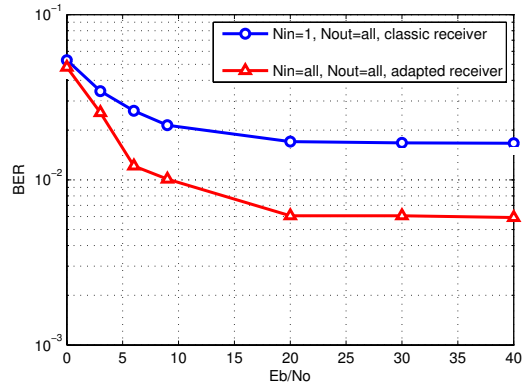

Fig. 5. BER vs. SNR with classic all-rake and adapted receiver in the cases of absence of TR ($N_{in} = 1, N_{out} = all$) and complete TR configuration ($N_{in} = all, N_{out} = all$)

[12] M. -G. Di Benedetto, G. Giancola. "Understanding Ultra Wide Band, Radio Fundamentals", Upper Saddle River, New Jersey: Prentice Hall Pearson Education, Inc., 2004.

[13] T. Strohmer, M. Emami, J. Hansen, G. Papanicolaou, and A. J. Paulraj, "Application of time-reversal with MMSE equalizer to UWB communications," in Proceedings of IEEE Global Telecommunications Conference (GLOBECOM '04), vol. 5, pp. 3123-3127, Dallas, Tex, USA, November-December 2004.

[14] J. Foerster. "Channel Modeling Sub-Committee Report Final", IEEE P802.15-02/490r1-SG3a, February 2003.

[15] D. Domenicali "Design of UWB Networks based on the application of the Cognitive Radio paradigm," PhD Thesis, 4 March 2008, Sapienza Universita di Roma/Universite Paris-Sud 11.

[16] M.Z. Win and R.A. Scholtz. "Ultra-Wide Bandwidth Time-Hopping Spread-Spectrum Impulse Radio for Wireless Multiple-Access Communications", IEEE Trans. on Com., vol.48, no.4, pp. 679-691, Oct. 2000.

[17] J. Fiorina and W. Hachem "On the Asymptotic Distribution of the Correlation Receiver Output for Time-Hopped UWB Signals," in IEEE Transactions on Signal Processing, Volume 54, Issue 7, July 2006 pp 2529 - 2545.

[18] J.Fiorina, D.Domenicali " The non validity of the gaussian approximation for multi-user interference in ultra wide band impulse radio: from an inconvenience to an advantage " IEEE Transactions on Wireless Communications, vol.8, November 2009, pages 5483-5489.

[6] Xiao,S. and Chen, J. and Liu,X. and Wang,B.-Z.,"Spatial focusing characteristics of time reversal UWB pulse transmission with different antenna arrays", Progress In Electromagnetics Research B, 2008,pp. 223-232,vol.2

[7] J. Fiorina, "A Simple IR-UWB Receiver Adapted to Multi-User Interferences" Globecom 2006, San Francisco, 27 Nov.-1 Dec.

[8] B. Mielczarek, M.O. Wessman and A. Svensson. "Performance of Coherent UWB Rake Receivers with Channel Estimators", Vehicular Technology Conference (VTC), Orlando, Florida, 6-9 Oct. 2003.

[9] A. Rajeswaran, V. S. Somayazulu and J. R. Foerster. "Rake Performance for a Pulse Based UWB System in a Realistic UWB Indoor Channel", IEEE International Conference on Communications (ICC), Anchorage, Alaska, USA, 11-15 May 2003.

[10] M. Z. Win and Z. A. Kostic. "Virtual path analysis of selective Rake receiver in dense multipath channels", IEEE Commun. Lett., Vol. 3, no. 11, pp. 308-310, Nov. 1999.

[11] D. Cassioli, M. Z. Win, F. Vatalaro, A. Molisch. "Performance of low-complexity rake reception in a realistic UWB channel", Proc. ICC 2002, pp. 763-767.